# Time-Domain Boundary Element Methods for the Neumann Problem: A Stable Formulation for Sound Emissions


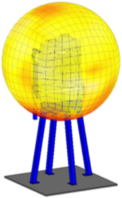

H. Gimperlein[1], B. Graf[2], C. Özdemir[1], K. Urban[3], S. Schneider[2,3]

1 - Engineering Mathematics, University of Innsbruck
2 - Structural Dynamics and Acoustics, Ulm University of Applied Sciences
3 - Institute of Numerical Mathematics, Ulm University

SIMAI 2025, SISSA, Trieste September 1-5

# From Challenges to Practical NVH Applications

*"Noise pollution, or sound pollution, is the propagation of noise or sound with potential harmful effects on humans and animals" (Senate Public Works, 1972)*.

**To address noise pollution**, it is essential to understand:

- **N**oise
- **V**ibration
- **H**arshness

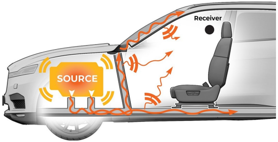


Source: ANSYS Blog – "Sources of NVH"

# From Challenges to Practical NVH Applications

*"Noise pollution, or sound pollution, is the propagation of noise or sound with potential harmful effects on humans and animals" (Senate Public Works, 1972)*.

**To address noise pollution**, it is essential to understand:

- **N**oise
- **V**ibration
- **H**arshness

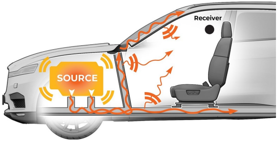


Source: ANSYS Blog – "Sources of NVH"

**State-of-the-Art** Numerical NVH Process:

**1** Structural Analysis

**Output:**
→ Natural frequencies
→ Mode shapes

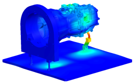

**2** Vibration Analysis (Typically in Time-Domain)

**Output:**
→ Structure-born sound

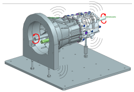

**3** Acoustic Analysis (Typically in Frequency-Domain)

**Output:**
→ Airborne sound

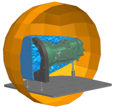

# Overview

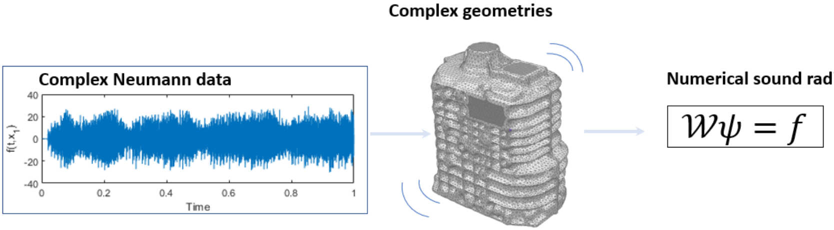


**In this talk:**

- Sound emission of complex geometries and Neumann data
- Convergence and stability of long-term simulations
- Numerical calculation for gearboxes and experimental validation

# Energetic Boundary Integral Equation for the Wave Equation

$u : \mathbb{R}^+ \times \Omega^+ \to \mathbb{R}$ sound pressure

$$\begin{cases} \partial_t^2 u - c^2 \Delta u = 0 & \text{in } \mathbb{R}^+ \times \Omega^+ \\ u = \partial_t u = 0 & \text{in } \mathbb{R}_0^- \times \Omega^+ \\ \partial_n u = f & \text{in } \mathbb{R}^+ \times \Gamma. \end{cases}$$

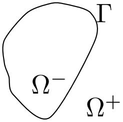


Fundamental solution of the wave equation in $\mathbb{R}^3$:

$$G(t,x) = \frac{\delta(t - |x|)}{4\pi|x|}.$$

# Energetic Boundary Integral Equation for the Wave Equation

$u : \mathbb{R}^+ \times \Omega^+ \to \mathbb{R}$ sound pressure

$$\begin{cases} \partial_t^2 u - c^2 \Delta u = 0 & \text{in } \mathbb{R}^+ \times \Omega^+ \\ u = \partial_t u = 0 & \text{in } \mathbb{R}_0^- \times \Omega^+ \\ \partial_n u = f & \text{in } \mathbb{R}^+ \times \Gamma. \end{cases}$$

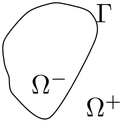


Fundamental solution of the wave equation in $\mathbb{R}^3$:

$$G(t,x) = \frac{\delta(t - |x|)}{4\pi|x|}.$$

**Double-layer potential ansatz:** $u = -D\,\psi$ in $\mathbb{R}^+ \times \Omega^+$,

$$\rightsquigarrow f(t,x) = \mathcal{W}\psi(t,x) := \int_{\mathbb{R}^+} \int_\Gamma \frac{\partial^2 G}{\partial_{n_y} \partial_{n_x}}(t-\tau, x-y)\,\psi(\tau,y)\ \ ds_y\, d\tau$$

# Space-Time Anisotropic Sobolev Spaces

Using the Fourier-Laplace transform, a space of distributions is introduced:

$$H^r_\sigma(\mathbb{R}^+, H^s(\Gamma)) := \left\{\psi \in \mathcal{D}'_+(H^s(\Gamma)) : e^{-\sigma t}\psi \in \mathcal{S}'_+(H^s(\Gamma)) \text{ and } ||\psi||_{r,s,\Gamma} < \infty\right\},$$

$$||\psi||_{r,s,\Gamma} := \left(\int_{\mathbb{R}+i\sigma}\int_\Gamma |\omega|^{2r}(|\omega|^2+|\eta|^2)^s|\mathcal{F}\psi(\omega,\eta)|^2 d\eta d\omega\right)^{1/2}.$$

## Space-Time Anisotropic Sobolev Spaces

Using the Fourier-Laplace transform, a space of distributions is introduced:

$$H^r_\sigma(\mathbb{R}^+, H^s(\Gamma)) := \left\{\psi \in \mathcal{D}'_+(H^s(\Gamma)) : e^{-\sigma t}\psi \in \mathcal{S}'_+(H^s(\Gamma)) \text{ and } ||\psi||_{r,s,\Gamma} < \infty\right\},$$

$$||\psi||_{r,s,\Gamma} := \left(\int_{\mathbb{R}+i\sigma}\int_\Gamma |\omega|^{2r}(|\omega|^2 + |\eta|^2)^s |\mathcal{F}\psi(\omega,\eta)|^2 d\eta d\omega\right)^{1/2}.$$

Space-time variational formulation of $\mathcal{W}\psi = f$ for $V := H^1_\sigma(\mathbb{R}^+, H^{1/2}(\Gamma))$:

$$\text{Find } \psi \in V \text{ s.t.} \quad \langle \mathcal{W}\psi, \partial_t \Psi\rangle_{\mathbb{R}^+\times\Gamma,\sigma} = \langle f, \partial_t \Psi\rangle_{\mathbb{R}^+\times\Gamma,\sigma} \quad \forall \Psi \in V.$$

### Theorem

*There exists a unique solution $\psi \in V$ such that for $f \in H^2_\sigma(\mathbb{R}^+, H^{-1/2}(\Gamma))$*

$$\|\psi\|_{1,1/2,\Gamma} \le C(\sigma)\|f\|_{2,-1/2,\Gamma}, \qquad \langle \mathcal{W}\psi, \partial_t\psi\rangle_{\mathbb{R}^+\times\Gamma,\sigma} \ge C(\sigma)\|\psi\|^2_{0,1/2,\Gamma}.$$

## Space-Time Anisotropic Sobolev Spaces

Using the Fourier-Laplace transform, a space of distributions is introduced:

$$H^r_\sigma(\mathbb{R}^+, H^s(\Gamma)) := \left\{\psi \in \mathcal{D}'_+(H^s(\Gamma)) : e^{-\sigma t}\psi \in \mathcal{S}'_+(H^s(\Gamma)) \text{ and } ||\psi||_{r,s,\Gamma} < \infty\right\},$$

$$||\psi||_{r,s,\Gamma} := \left(\int_{\mathbb{R}+i\sigma}\int_\Gamma |\omega|^{2r}(|\omega|^2 + |\eta|^2)^s |\mathcal{F}\psi(\omega,\eta)|^2 d\eta d\omega\right)^{1/2}.$$

Space-time variational formulation of $\mathcal{W}\psi = f$ for $V := H^1_\sigma(\mathbb{R}^+, H^{1/2}(\Gamma))$:

Find $\psi \in V$ s.t. $\langle \mathcal{W}\psi, \partial_t \Psi\rangle_{\mathbb{R}^+\times\Gamma,\sigma} = \langle f, \partial_t \Psi\rangle_{\mathbb{R}^+\times\Gamma,\sigma} \quad \forall \Psi \in V.$

### Theorem

*There exists a unique solution $\psi \in V$ such that for $f \in H^2_\sigma(\mathbb{R}^+, H^{-1/2}(\Gamma))$*

$$\|\psi\|_{1,1/2,\Gamma} \leq C(\sigma)\|f\|_{2,-1/2,\Gamma}, \qquad \langle \mathcal{W}\psi, \partial_t\psi\rangle_{\mathbb{R}^+\times\Gamma,\sigma} \geq C(\sigma)\|\psi\|^2_{0,1/2,\Gamma}.$$

Galerkin approximation: Find $\psi_{\Delta t,h} \in V_{\Delta t,h} \subset V$ s.t. $\forall \Psi_{\Delta t,h} \in V_{\Delta t,h}$:

$$\langle \mathcal{W}\psi_{\Delta t,h}, \partial_t \Psi_{\Delta t,h}\rangle_{\mathbb{R}^+\times\Gamma,\sigma} = \langle f, \partial_t \Psi_{\Delta t,h}\rangle_{\mathbb{R}^+\times\Gamma,\sigma}.$$

# Discretization

**Space**:

- $\Gamma = \bigcup_{i=1}^{N_s} \Gamma_i$ (quasi-uniform) triangulation
- $V_h^p$: space of piecewise polynomial functions of degree $p$ (continuous, if $p \geq 1$)

**Time**:

- $[0, T) = \bigcup_{n=1}^{N_t} I_n, \;\; I_n = [t_{n-1}, t_n), \;\; t_n = n\,\Delta t$
- $V_{\Delta t}^q$: space of piecewise polynomial functions of degree $q$ (continuous if $q \geq 1$)

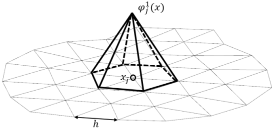


$\rightsquigarrow$ Tensor product in **space-time**: $V_{\Delta t,h}^{p,q} := V_{\Delta t}^q \times V_h^p$.

# Discretization

**Space**:

- $\Gamma = \bigcup_{i=1}^{N_s} \Gamma_i$ (quasi-uniform) triangulation
- $V_h^p$: space of piecewise polynomial functions of degree $p$ (continuous, if $p \geq 1$)

**Time**:

- $[0,T) = \bigcup_{n=1}^{N_t} I_n, \;\; I_n = [t_{n-1}, t_n), \;\; t_n = n\,\Delta t$
- $V_{\Delta t}^q$: space of piecewise polynomial functions of degree $q$ (continuous if $q \geq 1$)

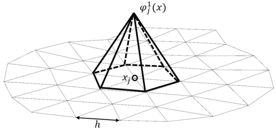


$\rightsquigarrow$ Tensor product in **space-time**: $V_{\Delta t,h}^{p,q} := V_{\Delta t}^q \times V_h^p$.

Using $\psi_{\Delta t,h}(t,x) = \sum_{i=1}^{N_t} \sum_{j=1}^{N_s} \alpha_j^i \varphi_j^1(x) \beta_j^1(t) \in V_{\Delta t,h}^{1,1}$ it follows:

$$\underbrace{\begin{pmatrix} W^0 & 0 & 0 & \cdots \\ W^1 & W^0 & 0 & \\ W^2 & W^1 & W^0 & \cdots \\ \vdots & & \vdots & \ddots \end{pmatrix}}_{=:\boldsymbol{W} \in \mathbb{R}^{N_t N_s \times N_t N_s}} \underbrace{\begin{pmatrix} \boldsymbol{\alpha}^1 \\ \boldsymbol{\alpha}^2 \\ \vdots \\ \boldsymbol{\alpha}^{N_t - 1} \end{pmatrix}}_{=:\boldsymbol{\alpha} \in \mathbb{R}^{N_t N_s}} = \underbrace{\begin{pmatrix} \boldsymbol{F}^1 \\ \boldsymbol{F}^2 \\ \vdots \\ \boldsymbol{F}^{N_t - 1} \end{pmatrix}}_{=:\boldsymbol{F} \in \mathbb{R}^{N_t N_s}}$$

# Marching-on-in-time algorithm (MOT)

Block forward substitution:

$$\forall n = 1, \dots, N_t : \sum_{m=1}^{n} W^{n-m} \boldsymbol{\alpha}^m = \boldsymbol{F}^n \Leftrightarrow W^0 \boldsymbol{\alpha}^n = \boldsymbol{F}^n - \sum_{m=1}^{n-1} W^{n-m} \boldsymbol{\alpha}^m.$$

For step $n$, two extra integrals (besides $W^{n-1}$):

$$\int\int_{E_{n-1}} \frac{n_x \cdot n_y \, \varphi_i(y) \varphi_j(x)}{4\pi |x-y| (\Delta t)} \, ds_y \, ds_x$$
$$+ \int\int_{E_{n-1}} \frac{(\mathrm{curl}_\Gamma \varphi_i)(y) \, (\mathrm{curl}_\Gamma \varphi_j)(x)}{4\pi |x-y| 2 (\Delta t)} (|x-y|^2 - 2|x-y| \, t_{n-1} + t_{n-1}^2) \, ds_y \, ds_x.$$

Light cone: $E_{n-1} := \{(x,y) \in \Gamma \times \Gamma : \ t_{n-1} \leq |x-y| \leq t_n\}$:

- $\rightsquigarrow$ Restrict the integration from $\Gamma \times \Gamma$ to $E_{n-1} \subset \Gamma \times \Gamma$
- $\rightsquigarrow$ Vanishes for $n - 1 > \left\lceil \frac{\mathrm{diam}(\Gamma)}{\Delta t} \right\rceil$

# More Boundary Integral Formulations

**Single-layer potential ansatz:** $u = S\,\varphi \rightsquigarrow (\mathcal{K}' - \frac{1}{2} Id)\varphi = f$
with $\mathcal{K}'\varphi := \int_{\mathbb{R}^+} \int_\Gamma \frac{\partial G}{\partial n_x}(t-\tau, x, y)\, \varphi(\tau, y)\, d\tau\, ds_y$.

Space-time Petrov-Galerkin approximation:
Find $\phi_{\Delta t,h} \in V^{0,0}_{\Delta t,h}$ s.t. $\forall \partial_t \Phi_{\Delta t,h} \in V^{0,0}_{\Delta t,h}$:

$$\langle (\mathcal{K}' - \tfrac{1}{2} Id)\phi_{\Delta t,h}, \partial_t \Phi_{\Delta t,h} \rangle_{\mathbb{R}^+ \times \Gamma, \sigma} = \langle f, \partial_t \Phi_{\Delta t,h} \rangle_{\mathbb{R}^+ \times \Gamma, \sigma}. \tag{1}$$

**Collocation based combined layer potential ansatz:** $u = -S\partial_n u^+ + Du^+$.
$\rightsquigarrow$ Approximate: $u$ linear in time and constant space, $f$ constant in time and space.

Semidiscretization leads to:

$$u_h^n(x_i) = -S_{\Delta t,h} \tfrac{1}{2} f_h^n(x_i) + D_{\Delta t,h} u_h^{n,+}(x_i) \tag{2}$$

# More Boundary Integral Formulations

**Single-layer potential ansatz:** $u = S\,\varphi \rightsquigarrow (\mathcal{K}' - \frac{1}{2}Id)\varphi = f$
with $\mathcal{K}'\varphi := \int_{\mathbb{R}^+}\int_\Gamma \frac{\partial G}{\partial n_x}(t-\tau, x, y)\,\varphi(\tau, y)\,d\tau\,ds_y$.

Space-time Petrov-Galerkin approximation:
Find $\phi_{\Delta t,h} \in V^{0,0}_{\Delta t,h}$ s.t. $\forall \partial_t \Phi_{\Delta t,h} \in V^{0,0}_{\Delta t,h}$:

$$\langle (\mathcal{K}' - \tfrac{1}{2}Id)\phi_{\Delta t,h}, \partial_t \Phi_{\Delta t,h}\rangle_{\mathbb{R}^+\times\Gamma,\sigma} = \langle f, \partial_t \Phi_{\Delta t,h}\rangle_{\mathbb{R}^+\times\Gamma,\sigma}. \tag{1}$$

**Collocation based combined layer potential ansatz:** $u = -S\partial_n u^+ + Du^+$.
$\rightsquigarrow$ Approximate: $u$ linear in time and constant space, $f$ constant in time and space.

Semidiscretization leads to:

$$u_h^n(x_i) = -S_{\Delta t,h}\tfrac{1}{2}f_h^n(x_i) + D_{\Delta t,h}u_h^{n,+}(x_i) \tag{2}$$

$\rightsquigarrow$ (1) and (2) lack stability estimates and are practically unstable!

# Convergence Investigation

Convergence of $\mathcal{W}\psi_{\Delta t,h} = f$ up to $T = 10$ for unit sphere

- Neumann boundary condition:

$$f(t,x) = \frac{\partial}{\partial r}\left\{\frac{r-t}{2r}\left(1+\cos\left(\frac{\pi(r-t)}{0.9}\right)\right)^2 H(0.9-|r-t|)\right\}\Bigg|_{r=1} \qquad (3)$$

- Discretization parameters:
  - Spatial: 20 up to 20480 elements, 12-10242 nodes
  - Time: $\Delta t = 2^{-1}$ up to $\Delta t = 2^{-6}$ $\rightsquigarrow \Delta t/h \approx 0.38$

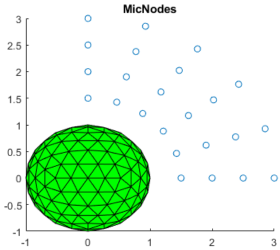

# Convergence Investigation

Convergence of $\mathcal{W}\psi_{\Delta t,h} = f$ up to $T = 10$ for unit sphere

- Neumann boundary condition:

$$f(t,x) = \frac{\partial}{\partial r}\left\{\frac{r-t}{2r}\left(1+\cos\left(\frac{\pi(r-t)}{0.9}\right)\right)^2 H(0.9-|r-t|)\right\}\Bigg|_{r=1} \qquad (3)$$

- Discretization parameters:
  - Spatial: 20 up to 20480 elements, 12-10242 nodes
  - Time: $\Delta t = 2^{-1}$ up to $\Delta t = 2^{-6}$ $\rightsquigarrow \Delta t/h \approx 0.38$

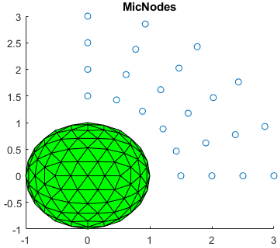


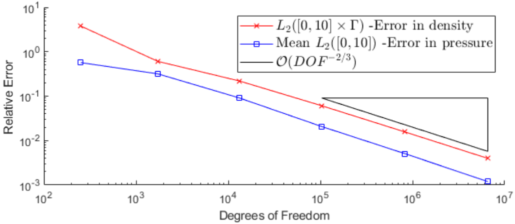

# Long-time Investigation

Stability of $\mathcal{W}\psi_{\Delta t,h} = f$ up to $T = 6800$, benchmarked against alternative methods:

- Two real-world housings of different complexity

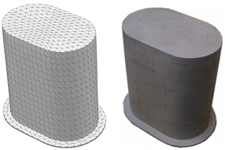

Oval Principal Gearbox Housing (OPG)

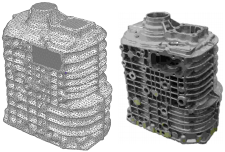

ZF Vehicle Gearbox Housing (ZFG)

- Neumann boundary condition (3)
- Discretization parameters:
  - OPG: $h = 22$, $1418$ nodes ( $2832$ elements)
  - ZFG: $h = 10$, $14351$ nodes ($28698$ elements)
  - $\Delta t/h$ ratios: $3.0$, $1.5$, ..., $0.1$

## OPG:

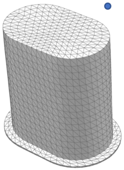

| No. | $\Delta t/h$ | $\Delta t$ | # timesteps | $\mathcal{W}$ | $\mathcal{K}'$ | Colloc. |
|---|---|---|---|---|---|---|
| 1 | **3** | $2^{-3.18}$ | 61608 | | | |
| 2 | **1.5** | $2^{-4.18}$ | 123216 | | | |
| 3 | **0.75** | $2^{-5.18}$ | 246500 | | | |
| 4 | **0.38** | $2^{-6.17}$ | 489668 | | | |
| 5 | **0.19** | $2^{-7.17}$ | 979268 | | | |
| 5.1 | 0.16 | $2^{-7.41}$ | 1156068 | | | |
| 5.2 | 0.13 | $2^{-7.71}$ | 1423784 | | | |
| 5.3 | 0.11 | $2^{-7.95}$ | 1681436 | | | |
| 6 | **0.10** | $2^{-8.09}$ | 1852796 | | | |

Stability Results for Different Grid Resolutions (OPG)

# OPG:

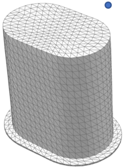

| No. | $\Delta t/h$ | $\Delta t$ | # timesteps | $\mathcal{W}$ | $\mathcal{K}'$ | Colloc. |
|---|---|---|---|---|---|---|
| 1 | **3** | $2^{-3.18}$ | 61608 | | | ✓ |
| 2 | **1.5** | $2^{-4.18}$ | 123216 | | | ✓ |
| 3 | **0.75** | $2^{-5.18}$ | 246500 | | | ✓ |
| 4 | **0.38** | $2^{-6.17}$ | 489668 | | | ✓ |
| 5 | **0.19** | $2^{-7.17}$ | 979268 | | | ✓ |
| 5.1 | 0.16 | $2^{-7.41}$ | 1156068 | | | ✗ |
| 5.2 | 0.13 | $2^{-7.71}$ | 1423784 | | | ✗ |
| 5.3 | 0.11 | $2^{-7.95}$ | 1681436 | | | ✗ |
| 6 | **0.10** | $2^{-8.09}$ | 1852796 | | | ✗ |

Stability Results for Different Grid Resolutions (OPG)

## OPG:

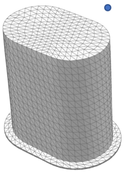

| No. | $\Delta t/h$ | $\Delta t$ | # timesteps | $\mathcal{W}$ | $\mathcal{K}'$ | Colloc. |
|---|---|---|---|---|---|---|
| 1 | **3** | $2^{-3.18}$ | 61608 | | ✓ | ✓ |
| 2 | **1.5** | $2^{-4.18}$ | 123216 | | ✓ | ✓ |
| 3 | **0.75** | $2^{-5.18}$ | 246500 | | ✓ | ✓ |
| 4 | **0.38** | $2^{-6.17}$ | 489668 | | ✓ | ✓ |
| 5 | **0.19** | $2^{-7.17}$ | 979268 | | ✓ | ✓ |
| 5.1 | 0.16 | $2^{-7.41}$ | 1156068 | | ✓ | ✗ |
| 5.2 | 0.13 | $2^{-7.71}$ | 1423784 | | ✓ | ✗ |
| 5.3 | 0.11 | $2^{-7.95}$ | 1681436 | | ✓ | ✗ |
| 6 | **0.10** | $2^{-8.09}$ | 1852796 | | ✓ | ✗ |

Stability Results for Different Grid Resolutions (OPG)

# OPG:

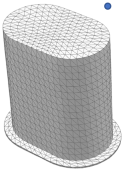

| No. | $\Delta t/h$ | $\Delta t$ | # timesteps | $\mathcal{W}$ | $\mathcal{K}'$ | Colloc. |
|---|---|---|---|---|---|---|
| 1 | **3** | $2^{-3.18}$ | 61608 | ✓ | ✓ | ✓ |
| 2 | **1.5** | $2^{-4.18}$ | 123216 | ✓ | ✓ | ✓ |
| 3 | **0.75** | $2^{-5.18}$ | 246500 | ✓ | ✓ | ✓ |
| 4 | **0.38** | $2^{-6.17}$ | 489668 | ✓ | ✓ | ✓ |
| 5 | **0.19** | $2^{-7.17}$ | 979268 | ✓ | ✓ | ✓ |
| 5.1 | 0.16 | $2^{-7.41}$ | 1156068 | ✓ | ✓ | ✗ |
| 5.2 | 0.13 | $2^{-7.71}$ | 1423784 | ✓ | ✓ | ✗ |
| 5.3 | 0.11 | $2^{-7.95}$ | 1681436 | ✓ | ✓ | ✗ |
| 6 | **0.10** | $2^{-8.09}$ | 1852796 | ✓ | ✓ | ✗ |

Stability Results for Different Grid Resolutions (OPG)

# OPG:

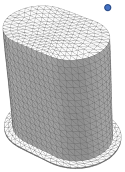

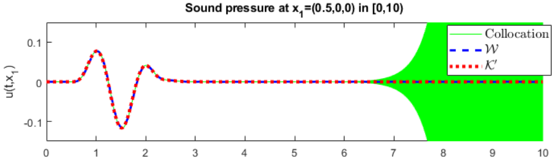


$u(t, x_1)$ for Case 5.1

| No. | $\Delta t/h$ | $\Delta t$ | # timesteps | $\mathcal{W}$ | $\mathcal{K}'$ | Colloc. |
|---|---|---|---|---|---|---|
| 1 | **3** | $2^{-3.18}$ | 61608 | ✓ | ✓ | ✓ |
| 2 | **1.5** | $2^{-4.18}$ | 123216 | ✓ | ✓ | ✓ |
| 3 | **0.75** | $2^{-5.18}$ | 246500 | ✓ | ✓ | ✓ |
| 4 | **0.38** | $2^{-6.17}$ | 489668 | ✓ | ✓ | ✓ |
| 5 | **0.19** | $2^{-7.17}$ | 979268 | ✓ | ✓ | ✓ |
| 5.1 | 0.16 | $2^{-7.41}$ | 1156068 | ✓ | ✓ | ✗ |
| 5.2 | 0.13 | $2^{-7.71}$ | 1423784 | ✓ | ✓ | ✗ |
| 5.3 | 0.11 | $2^{-7.95}$ | 1681436 | ✓ | ✓ | ✗ |
| 6 | **0.10** | $2^{-8.09}$ | 1852796 | ✓ | ✓ | ✗ |

Stability Results for Different Grid Resolutions (OPG)

## OPG:

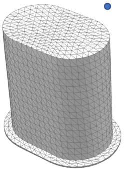

⇝ However: $\mathcal{K}'$ becomes unstable for slightly different meshes

| No. | $\Delta t/h$ | $\Delta t$ | # timesteps | $\mathcal{W}$ | $\mathcal{K}'$ | Colloc. |
|---|---|---|---|---|---|---|
| 1 | **3** | $2^{-3.18}$ | 61608 | ✓ | ✓ | ✓ |
| 2 | **1.5** | $2^{-4.18}$ | 123216 | ✓ | ✓ | ✓ |
| 3 | **0.75** | $2^{-5.18}$ | 246500 | ✓ | ✓ | ✓ |
| 4 | **0.38** | $2^{-6.17}$ | 489668 | ✓ | ✓ | ✓ |
| 5 | **0.19** | $2^{-7.17}$ | 979268 | ✓ | ✓ | ✓ |
| 5.1 | 0.16 | $2^{-7.41}$ | 1156068 | ✓ | ✓ | ✗ |
| 5.2 | 0.13 | $2^{-7.71}$ | 1423784 | ✓ | ✓ | ✗ |
| 5.3 | 0.11 | $2^{-7.95}$ | 1681436 | ✓ | ✓ | ✗ |
| 6 | **0.10** | $2^{-8.09}$ | 1852796 | ✓ | ✓ | ✗ |

Stability Results for Different Grid Resolutions (OPG)

## ZFG:

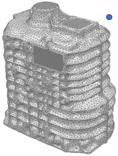

| No. | $\Delta t/h$ | $\Delta t$ | # timesteps | $\mathcal{W}$ | $\mathcal{K}'$ | Colloc. |
|---|---|---|---|---|---|---|
| 1 | **3** | $2^{-4.52}$ | 156000 | | | |
| 2 | **1.5** | $2^{-5.52}$ | 312000 | | | |
| 3 | **0.75** | $2^{-6.52}$ | 624100 | | | |
| 4 | **0.38** | $2^{-7.50}$ | 1230900 | | | |
| 5 | **0.19** | $2^{-9.50}$ | 2461900 | | | |
| 6 | **0.10** | $2^{-9.43}$ | 4690500 | | | |

Stability Results for Different Grid Resolutions (ZFG)

**ZFG:**

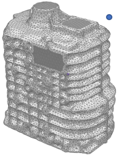

| No. | $\Delta t/h$ | $\Delta t$ | # timesteps | $\mathcal{W}$ | $\mathcal{K}'$ | Colloc. |
|---|---|---|---|---|---|---|
| 1 | **3** | $2^{-4.52}$ | 156000 | | ✗ | ✗ |
| 2 | **1.5** | $2^{-5.52}$ | 312000 | | ✗ | ✗ |
| 3 | **0.75** | $2^{-6.52}$ | 624100 | | ✗ | ✗ |
| 4 | **0.38** | $2^{-7.50}$ | 1230900 | | ✗ | ✗ |
| 5 | **0.19** | $2^{-9.50}$ | 2461900 | | ✗ | ✗ |
| 6 | **0.10** | $2^{-9.43}$ | 4690500 | | ✗ | ✗ |

Stability Results for Different Grid Resolutions (ZFG)

## ZFG:

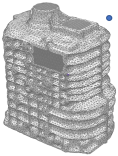

| No. | $\Delta t/h$ | $\Delta t$ | # timesteps | $\mathcal{W}$ | $\mathcal{K}'$ | Colloc. |
|---|---|---|---|---|---|---|
| 1 | **3** | $2^{-4.52}$ | 156000 | ✓ | ✗ | ✗ |
| 2 | **1.5** | $2^{-5.52}$ | 312000 | ✓ | ✗ | ✗ |
| 3 | **0.75** | $2^{-6.52}$ | 624100 | ✓ | ✗ | ✗ |
| 4 | **0.38** | $2^{-7.50}$ | 1230900 | ✓ | ✗ | ✗ |
| 5 | **0.19** | $2^{-9.50}$ | 2461900 | ✓ | ✗ | ✗ |
| 6 | **0.10** | $2^{-9.43}$ | 4690500 | | ✗ | ✗ |

Stability Results for Different Grid Resolutions (ZFG)

## ZFG:

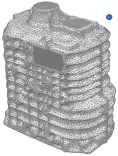

Key Findings:

- Collocation: unstable for small $\Delta t/h$ and complex $\Gamma$
- $\mathcal{K}'$: unpredictable stability
- $\mathcal{W}$: robust across all tests

| No. | $\Delta t/h$ | $\Delta t$ | # timesteps | $\mathcal{W}$ | $\mathcal{K}'$ | Colloc. |
|---|---|---|---|---|---|---|
| 1 | **3** | $2^{-4.52}$ | 156000 | ✓ | ✗ | ✗ |
| 2 | **1.5** | $2^{-5.52}$ | 312000 | ✓ | ✗ | ✗ |
| 3 | **0.75** | $2^{-6.52}$ | 624100 | ✓ | ✗ | ✗ |
| 4 | **0.38** | $2^{-7.50}$ | 1230900 | ✓ | ✗ | ✗ |
| 5 | **0.19** | $2^{-9.50}$ | 2461900 | ✓ | ✗ | ✗ |
| 6 | **0.10** | $2^{-9.43}$ | 4690500 | | ✗ | ✗ |

Stability Results for Different Grid Resolutions (ZFG)

# Application of $\mathcal{W}$: Harmonic Sound Radiation of the OPG

**Experimental Setup:**

- Environmentally decoupled
- Accelerometers for vibration
- Microphones for sound pressure
- Excitation: 376.175 Hz

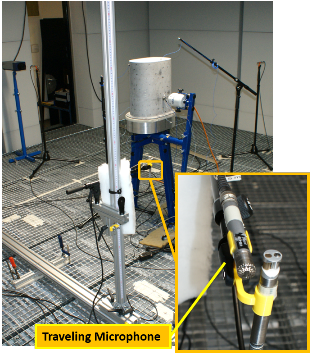

# Application of $\mathcal{W}$: Harmonic Sound Radiation of the OPG

**Experimental Setup:**

- Environmentally decoupled
- Accelerometers for vibration
- Microphones for sound pressure
- Excitation: 376.175 Hz

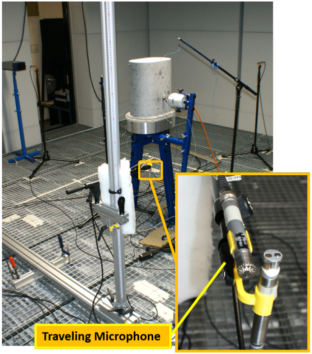


**Numerical Setup:**

- Nodes = 4876
- $\Delta t = 1/25600$ seconds
- $T = [0, 3)$ seconds
- $f = -\rho\, c^2 \partial_{tt}\, s(t, x)$

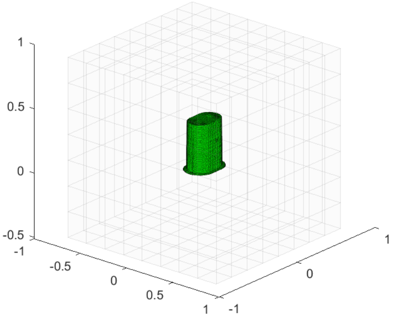

# Application of $\mathcal{W}$: Harmonic Sound Radiation of the OPG

**Experimental Setup:**

- Environmentally decoupled
- Accelerometers for vibration
- Microphones for sound pressure
- Excitation: 376.175 Hz

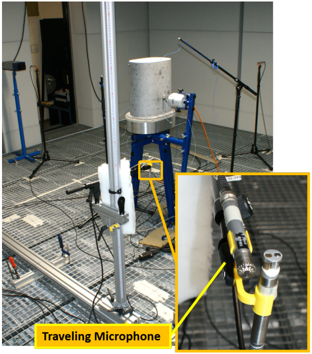


**Numerical Setup:**

- Nodes = 4876
- $\Delta t = 1/25600$ seconds
- $T = [0, 3)$ seconds
- $f = -\rho\, c^2 \partial_{tt}\, s(t, x)$

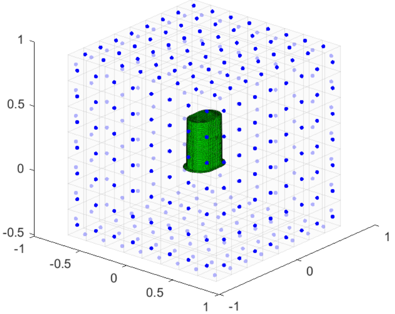

Sound pressure level $$||u(t,x_i)||^{dB}_{L_2(T)} := 10\log\left[\frac{1}{T}\frac{\|u(t,x_i)\|^2_{L_2(T)}}{u_0^2}\right]$$

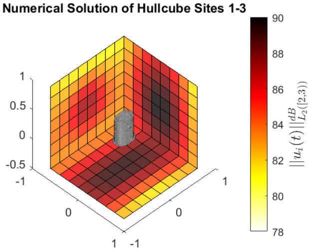


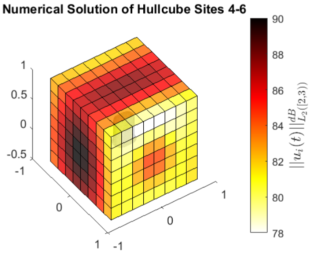


$$||u_{\mathcal{W}}(t,x)||^{dB}_{L_2([2,3],\partial H)} = 85.39\,\mathrm{dB}$$

Sound pressure level $$||u(t,x_i)||^{dB}_{L_2(T)} := 10 \log \left[ \frac{1}{T} \frac{\|u(t,x_i)\|^2_{L_2(T)}}{u_0^2} \right]$$

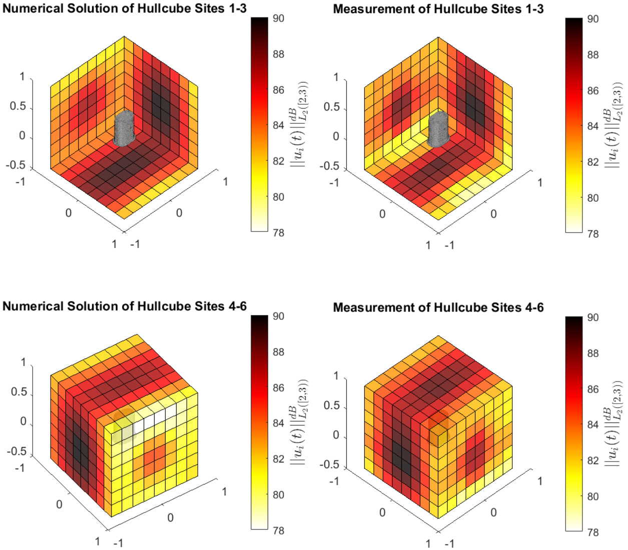


$$||u_{\mathcal{W}}(t,x)||^{dB}_{L_2([2,3],\partial H)} = 85.39\,\text{dB} \qquad ||u_M(t,x)||^{dB}_{L_2([2,3],\partial H)} = 85.14\,\text{dB}$$

# Application of $\mathcal{W}$: Transient Sound Radiation of the ZFG

**Experimental Setup:**

- Accelerometers and microphones
- Random excitation force

Neumann data $f = -\rho\, c^2 \partial_{tt}\, s(t,x)$ extracted by dynamic analysis:

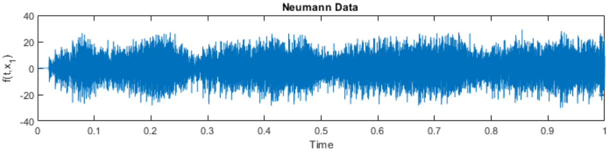


**Numerical Setup**

- Nodes $= 14351$
- $\Delta t = 51200^{-1}$ seconds
- $T = [0,1)$ seconds
- 11 microphone points

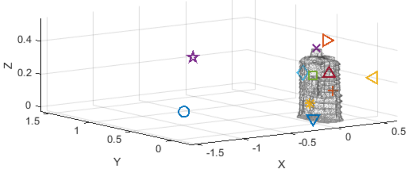

# Application of $\mathcal{W}$: Transient Sound Radiation of the ZFG

**Experimental Setup:**

- Accelerometers and microphones
- Random excitation force

Neumann data $f = -\rho\, c^2 \partial_{tt} s(t,x)$ extracted by dynamic analysis:

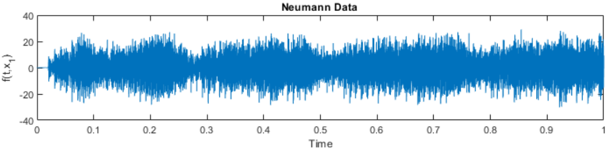


**Numerical Setup**

- Nodes $= 14351$
- $\Delta t = 51200^{-1}$ seconds
- $T = [0,1)$ seconds
- 11 microphone points

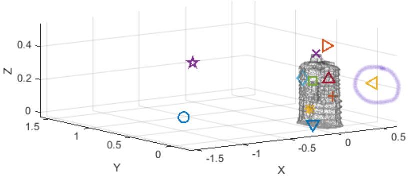

**Time-domain** results for $u_{10}(t)$:

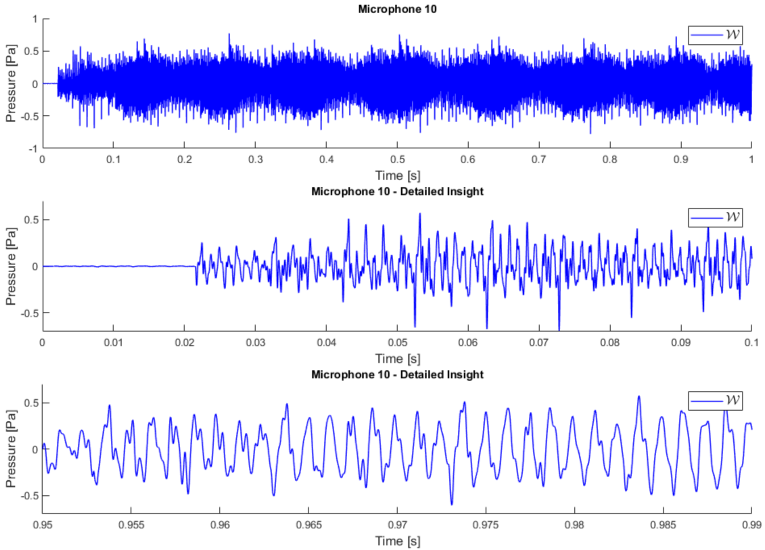

**Time-domain** results for $u_{10}(t)$:

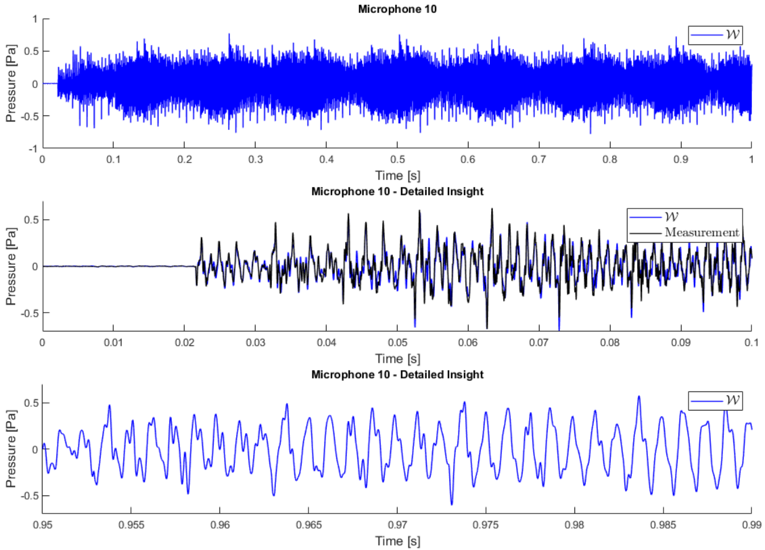

**Time-domain** results for $u_{10}(t)$:

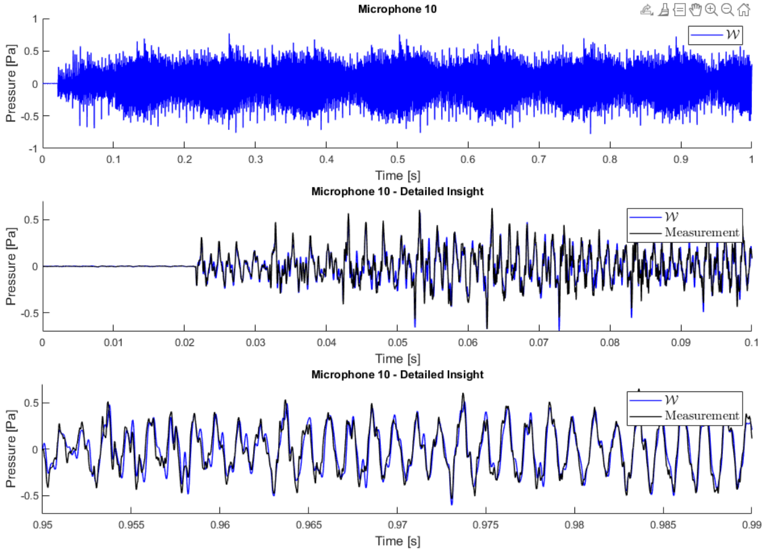

**Frequency-domain** results for $\mathcal{F}(u_{10}(t))$:

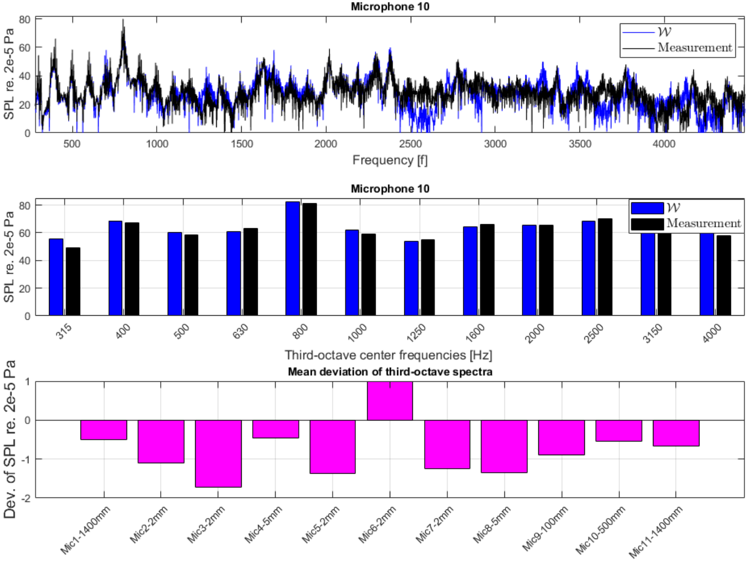

# Conclusions and Outlook

- $\mathcal{W}\psi = f$ robust for long-term simulations
- Standard collocation and $\mathcal{K}'$ formulation unstable for small $\Delta t/h$ or complex geometries
- Good agreement with experiments (OPG / ZFG)
- Outlook: Model order reduction for practical NVH applications